

DNA-PKcs, Allostery, and DNA Double-Strand Break Repair: Defining the Structure and Setting the Stage

Dimitri Y. Chirgadze, David B. Ascher¹, Tom L. Blundell²,
Bancinyane L. Sibanda

University of Cambridge, Cambridge, United Kingdom

²Corresponding author: e-mail address: tlb20@cam.ac.uk

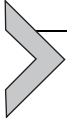
Contents

1. Introduction	146
2. Defining the Structure of DNA-PKcs	148
3. Exploiting Multiple Se-Met Substitutions	148
4. Using Se-Met Sites to Check Sequence Registration	151
5. DNA-PKcs as a Stage for the Assembly of the Actors in NHEJ	152
Acknowledgments	155
References	155

Abstract

DNA-dependent protein kinase catalytic subunit (DNA-PKcs) is central to the regulation of the DNA damage response and repair through nonhomologous end joining. The structure has proved challenging due to its large size and multiple HEAT repeats. We have recently reported crystals of selenomethionine-labeled DNA-PKcs complexed with native KU80ct₁₉₄ (KU80 residues 539–732) diffracting to 4.3 Å resolution. The novel use of crystals of selenomethionine-labeled protein expressed in HeLa cells has facilitated the use of single anomalous X-ray scattering of this 4128 amino acid, multiple HEAT-repeat structure. The monitoring of the selenomethionines in the anomalous-difference density map has allowed the checking of the amino acid residue registration in the electron density, and the labeling of the Ku-C-terminal moiety with selenomethionine has further allowed its identification in the structure of the complex with DNA-PKcs. The crystal structure defines a stage on which many of the components assemble and regulate the kinase activity through modulating the conformation and allosteric regulation of kinase activity.

¹ Present address: Department of Biochemistry and Molecular Biology, University of Melbourne, 30 Flemington Road, Parkville, 3052, Australia.



1. INTRODUCTION

The DNA-dependent protein kinase catalytic subunit (DNA-PKcs; Gell & Jackson, 1999), a giant single-chain protein of 4128 amino acids, plays a central role in the regulation of DNA damage response and repair through nonhomologous end joining (NHEJ) (Lieber, 2010; O'Driscoll & Jeggo, 2006). It allows DNA double-strand breaks to be repaired promptly when a sister chromatid is unavailable (Critchlow & Jackson, 1998), a process used also in V(D)J recombination (Schatz, 2004). DNA-PKcs autophosphorylation (Chen et al., 2005) and binding to the KU70/80 heterodimer (Walker, Corpina, & Goldberg, 2001) set the stage for assembly of the main actors in NHEJ, which include Artemis, XRCC4, XRCC4/DNA ligase IV, XLF, and PAXX (Lieber, 2010; Ochi et al., 2015).

In the NHEJ process, DNA-PKcs with Ku70/Ku80 heterodimers regulate in space and time a complex series of events: synapsis, end processing, and ligation (Lieber, 2010). During synapsis, Ku70/Ku80 heterodimers assemble around and maintain proximity of broken DNA ends (Walker et al., 2001). DNA-PKcs (PI3-kinase-related serine/threonine kinase) is recruited through interaction with Ku80 C-terminus (Gell & Jackson, 1999; Singleton, Torres-Arzayus, Rottinghaus, Taccioli, & Jeggo, 1999). Two DNA-PKcs complexes hold DNA ends close together (Spagnolo, Rivera-Calzada, Pearl, & Llorca, 2006). DNA-PKcs phosphorylates itself and various other proteins, including NHEJ components. End processing involves nucleases such as Artemis, which exhibits 5' to 3' endonuclease activity after activation by DNA-PKcs phosphorylation (Moshous et al., 2001). The final ligation step is mediated by DNA ligase IV (LigIV) in a stable complex with dimeric XRCC4 (Grawunder et al., 1997). XLF/Cernunnos also interacts with XRCC4 and enhances LigIV DNA ligation (Buck et al., 2006).

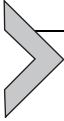
Knowledge of the structures of individual molecules and their complexes over space and time is required in order to understand this complex multi-step system, the details of which will depend on the location of the DNA damage and the nature of the DNA broken ends. Structures of many individual components such as LigIV (Ochi et al., 2010, 2012) and XLF (Li et al., 2008), as well as binary complexes of XLF-XRCC4 (Hammel et al., 2011; Wu et al., 2011), LigIV-Artemis (Ochi, Gu, & Blundell, 2013), and XRCC4-LigIV (Sibanda et al., 2001) have been reported. On the other

hand, structural information on DNA-PKcs has been limited to our low-resolution (6.6 Å) crystal structure (Sibanda, Chirgadze, & Blundell, 2010) and to lower resolution cryo-EM structures (>13 Å) (Chiu, Cary, Chen, Peterson, & Stewart, 1998; Leuther, Hammarsten, Kornberg, & Chu, 1999; Rivera-Calzada, Maman, Spagnolo, Pearl, & Llorca, 2005; Williams, Lee, Shi, Chen, & Stewart, 2008).

The structure of DNA-PKcs has proved challenging due to its large size and multiple HEAT (Huntingtin, Elongation Factor 3, PP2 A, and TOR1) repeats (Fig. 1). We have recently reported crystals of selenomethionine (Se-Met)-labeled DNA-PKcs complexed with native KU80_{ct194} (KU80 residues 539–732) diffracting to 4.3 Å resolution (Sibanda, Chirgadze, Ascher, & Blundell, 2017). We have exploited anomalous scattering through substitution of Se-Met. Although this is an established technique it had not been previously used to our knowledge with HeLa cell expression, in our case leading to identification of 213 Se-Mets in ordered regions of the two molecules of the asymmetric unit. A particularly useful aspect of this approach in interpreting our 4.3 Å resolution electron density of DNA-PKcs was to check sequence registration in a structure that has over 80 HEAT repeats and other helix-turn-helix motifs in the 4128 amino acids in each polypeptide chain in the asymmetric unit—the longest single-chain protein yet deposited in the PDB. This aspect of the analysis reported in *Science* (Sibanda et al., 2017) may be of value in other long single-chain molecules of the PI3-kinase family and elsewhere in cell regulatory systems and is the focus of this review.

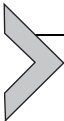


Fig. 1 Schematic of the overall sequence and structural units of DNA-PKcs. N-terminal in *blue*, Circular Cradle in *green*, Head comprising FAT region in *yellow*, kinase in *red*, and the FATC in *light pink*. The sequence of domains is compared to other PI3-K family members, TRRAP (transformation/transcription domain-associated protein), mTOR (mammalian target of rapamycin), ATM (ataxia-telangiectasia mutated), ATR (ATM and Rad3 related), SMG1 (human suppressor of morphogenesis in genitalia). *Figure adapted from fig. 1 published in Sibanda, B.L., Chirgadze, D.Y., Ascher, D.B., Blundell, T.L. (2017). DNA-PKcs structure suggests an allosteric mechanism modulating DNA double-strand break repair. Science, 355(6324), 520–524. [http://dx.doi.org/10.1126/science.aak9654].*



2. DEFINING THE STRUCTURE OF DNA-PKcs

DNA-PKcs was isolated from HeLa cells using a modification of the purification protocol of Gell and Jackson (1999) as described in Sibanda et al. (2017). DNA-PKcs was purified in the presence of 0.5–5 mM EDTA to prevent autophosphorylation. Heavy metal ion solutions, the best of which was involved the dodeca- μ -bromo-hexatantalum cation ($\text{Ta}_6\text{Br}_{12}^{2+}$) as a bromide salt, were used to form crystals for isomorphous replacement but the resulting crystals were less well ordered. However, the use of multiple-wavelength anomalous dispersion allowed determination of the molecular structure of DNA-PKcs:Ku80ct₁₉₄ complex at ~ 6.6 Å resolution (Sibanda et al., 2010). This has subsequently been improved (to 6.4 Å) using multicrystal anomalous diffraction analysis for low-resolution macromolecular phasing in a method pioneered by Hendrickson et al. (Liu, Zhang, & Hendrickson, 2011). However, the presence of large variations in cell parameters, due to soaking of $\text{Ta}_6\text{Br}_{12}^{2+}$, significantly reduced the number of datasets that could be used.



3. EXPLOITING MULTIPLE SE-MET SUBSTITUTIONS

For this reason, we decided to explore the use of Se-Met-labeled DNA-PKcs and Ku80ct₁₉₄ proteins. In order to produce Se-Met-labeled proteins in HeLa cells, we designed a modified expression protocol based upon the procedure used in baculovirus-infected Sf21 cells to produce recombinant Se-Met-labeled proteins (Bellizzi, Widom, Kemp, & Clardy, 1999). HeLa cells were grown in a medium that was methionine free, and this was used as a stock solution to grow for 4 h a larger volume in methionine-free medium, in order to exhaust intracellular pools of methionine. Cell pellets were formed by gentle spinning and resuspension in methionine-free medium, before increasing volumes using methionine-free medium. L-Se-Met was then introduced and cells grown to the normal cell density, before harvesting and processing as for native cells. CR-UK provided the first small batch of these cells. The second batch was supplied by Helmholtz-Zentrum who selected appropriate conditions to maximize cell growth. The Se-Met protein was purified in the same way as the native protein. We also produced Ku80ct₁₉₄ substituted with Se-Met in *Escherichia coli* cells (BL21 DE3) using approaches described earlier (Sibanda et al., 2010). The crystals of complexes of the wildtype and Se-Met-substituted

proteins were produced by vapor-diffusion with hanging drops. Fourteen Se-Met datasets were chosen from over one hundred collected from ESRF beamline ID29/ID23 (Grenoble, France) that diffracted to around 4.5 Å resolution. The use of Se-Met-labeled DNA-PKcs complexed with wildtype Ku80ct₁₉₄ domain gave less variation in crystal dimensions and better diffraction varying between 4.0 and 5.0 Å.

Selenium sites were identified using the anomalous difference maps using phases calculated from the multicrystal Ta₆Br₁₂²⁺ derivative datasets. Each DNA-PKcs molecule of the model was placed in the asymmetric unit of the multicrystal datasets using molecular replacement and the phases were calculated in the PHENIX software suite (Adams et al., 2010). Areas in the anomalous difference maps with sigma levels above four were considered to be possible selenium sites (Fig. 2). The best anomalous difference maps were calculated from the datasets from 14 single crystals of the selenium sites merged at 4.9 and 4.3 Å resolutions. The multicrystal dataset at 4.3 Å allowed a total of 172 of the expected 236 selenium sites to be identified, with good consistency between the two molecules in the asymmetric unit (Fig. 3). The electron-density maps were subjected to density modification including twofold noncrystallographic symmetry averaging of the density for the

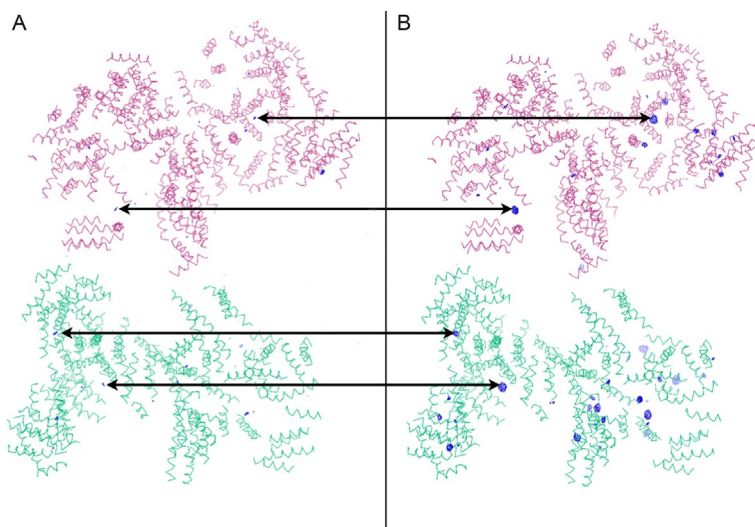


Fig. 2 Comparison of the anomalous difference maps calculated using: (A) a multicrystal dataset that has only two single-crystal datasets and (B) a multicrystal dataset that has 14 single-crystal datasets. The figure shows the increase in sigma level of the areas of electron-density map (*blue* chicken-wire mesh) corresponding to the selenium atom sites, indicated by *white arrows*. Both maps are contoured at 4σ level.

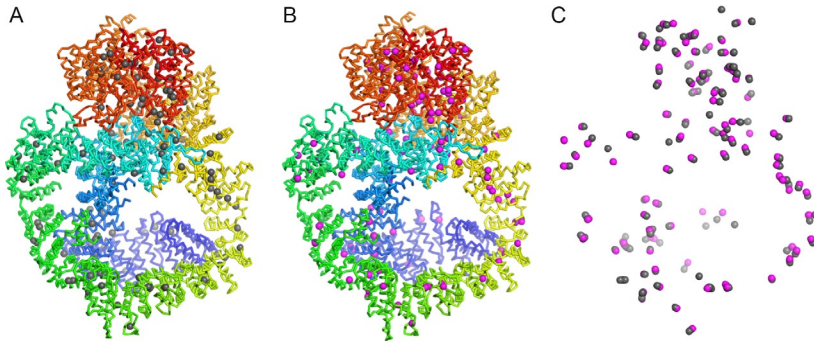


Fig. 3 The positions of selenium sites in the two molecules of DNA-PKcs of the asymmetric unit. The molecules of DNA-PKcs are shown as *ribbons in rainbow color*, from N-terminus—*blue* to C-terminus—*red*. The Se atoms are shown as either *gray* or *magenta spheres*. A total of 213 selenium sites of the 236 possible sites can be identified. Molecule A (A) has 109 sites, while molecule B (B) has 104. Superposition of molecules A and B is shown in (C) in order to demonstrate the correlation between the sites observed in both molecules. There are 104 pairs, comprising 208 sites of the two molecules in the asymmetric unit. *Figure adapted from fig. S8, published in Sibanda, B.L., Chirgadze, D.Y., Ascher, D.B., Blundell, T.L. (2017). DNA-PKcs structure suggests an allosteric mechanism modulating DNA double-strand break repair. Science, 355(6324), 520–524. [http://dx.doi.org/10.1126/science.aak9654].*

two molecules in the asymmetric unit using the SOLVE/RESOLVE routine of PHENIX software suite (Adams et al., 2010).

The new maps produced showed helical features including electron density corresponding to amino acid side chains. An example of an experimental electron-density map from this multocrystal dataset 6 at 4.3 Å resolution is shown in Fig. 4. The maps revealed more helices and the density in the loop regions of HEAT repeats, making it possible to trace the chain from the N- to the C-terminus. The model was manually rebuilt, corrected, and extended further; the resulting phases were used in a recalculation of the anomalous difference maps, which allowed identification of further selenium sites. Iteration of the process allowed 213 sites representing 90.0% of the possible number of sites to be identified. The structures of the two molecules were further refined exploiting rigid body and translation/libration/screw refinement, using the PHENIX software suite (Adams et al., 2010). Side-chains were modeled in an iterative process using Andante (Smith, Lovell, Burke, Montalvo, & Blundell, 2007) and Arpeggio (Jubb et al., 2017). The final R and R_{free} values are 38.6% and 43.7%, respectively. Structure evaluation and validation were performed using VADAR (Willard et al., 2003) for analysis of coordinates, packing, H-bonds, secondary

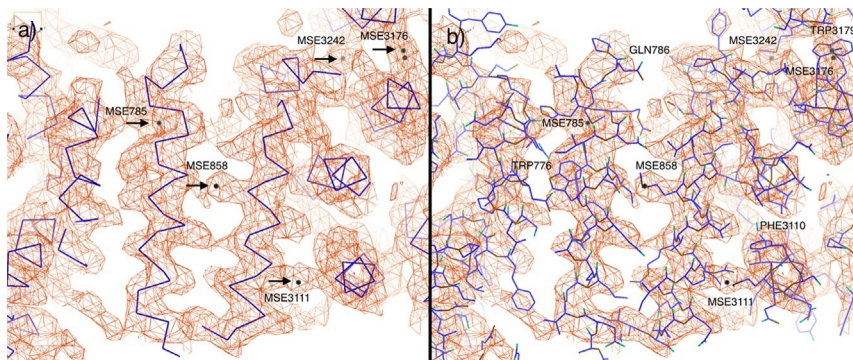


Fig. 4 Examples of electron-density maps in the vicinity of some of the Se-Met residues: (A) Experimental electron-density map obtained using the SAD technique with the multicrystal dataset at 4.3 Å resolution. The map is contoured at 1.0 σ level. The positions of selenium atoms are shown as white spheres and marked by arrows and residue numbers. The C-alpha trace of α -helices of DNA-PKcs is shown, while in (B) the side-chains of the corresponding area are shown. Figure adapted from fig. S9, published in Sibanda, B.L., Chirgadze, D.Y., Ascher, D.B., Blondell, T.L. (2017). DNA-PKcs structure suggests an allosteric mechanism modulating DNA double-strand break repair. *Science*, 355(6324), 520–524. [<http://dx.doi.org/10.1126/science.aak9654>].

structure and geometry, Verify_3D (Bowie, Luthy, & Eisenberg, 1991) and Harmony (<http://caps.ncbs.res.in/harmony/>) to look at the compatibility between the sequence and 3D structure.

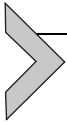
The Ku C-terminal region was identified from an anomalous difference map calculated using the cocrystals with the Se-Met derivatized Ku80ct₁₉₄. These showed only two areas where the density level was more than 3.5 σ consistent between the two molecules of DNA-PKcs present in the asymmetric unit. These were in unexplained electron density, locating the Ku-binding site A near α -helices 2012–2024 and 2059–2066. The anomalous difference map, taken together with the refined DNA-PKcs model, indicated that the Se-Met identified from the map is that in the C-terminal region of Ku that folds as a helix onto the DNA-PKcs (Sibanda et al., 2017) and that the globular helical region identified earlier by NMR is not ordered in the complex.



4. USING SE-MET SITES TO CHECK SEQUENCE REGISTRATION

The positions of selenium atoms were then used to identify methionine residues and to check the registration with the sequence. Eight

selenium sites were in disordered regions of the chain lacking good electron density. The even spacing of the Se-Met residues in the sequence allowed them to map the overall shape of the molecule (Figs. 3 and 4).



5. DNA-PKcs AS A STAGE FOR THE ASSEMBLY OF THE ACTORS IN NHEJ

The analysis of the structure of DNA-PKcs shows that it is assembled as three well defined, large structural units, within which motifs resembling HEAT repeats give rise to supersecondary structures with continuous hydrophobic cores (Fig. 5) (Sibanda et al., 2017). The structural units comprise the N-terminal region (38 α -helices, residues 1–892, four supersecondary structures: N1–N4), the Circular Cradle (85 α -helices, residues 893–2801; five supersecondary structures: CC1–CC5), and the C-terminal Head (64 α -helices, residues 2802–4128, FAT, FRB, kinase, and FATC).

The N-terminal region and the CC region of DNA-PKcs in particular are composed predominantly of HEAT repeats (Fig. 6). The regular repetitive nature of these HEAT-repeat supersecondary structures leads to some repetitive nature in the sequence, making sequence registration at medium to low resolution very difficult. The positioning of the Se-Met groups across these helices provided the necessary information to define their sequence register.

Although the findings of Weterings et al. (2009) indicate that the C-terminus of KU80 is not absolutely required for activation of DNA-PKcs, our structure indicates that it likely facilitates DNA-PKcs recruitment. Comparison with the cryo-EM maps of the DNA-PKcs–Ku70/80 complex (Spagnolo et al., 2006) reveals that density for Ku70/80 complex is located close to CC4 and N1 (Fig. 5). N1–N3 of DNA-PKcs is found to mediate DNA binding (Douglas et al., 2007; Hammel et al., 2010; Meek, Lees-Miller, & Modesti, 2012; Spagnolo et al., 2006; Villarreal & Stewart, 2014; Williams et al., 2008). This region, together with the Circular Cradle, forms a ring at the base of the molecule through which KU70/80 may present DNA for repair, and binding of Ku or DNA likely activates the allosteric mechanism needed for the N-terminal and Circular Cradle to communicate with the kinase in the Head (Sibanda et al., 2017).

In NHEJ, appropriate spatial colocalization of components is assured by collocation on DNA-PKcs, which may be considered as a stage where the main actors gather and engage.

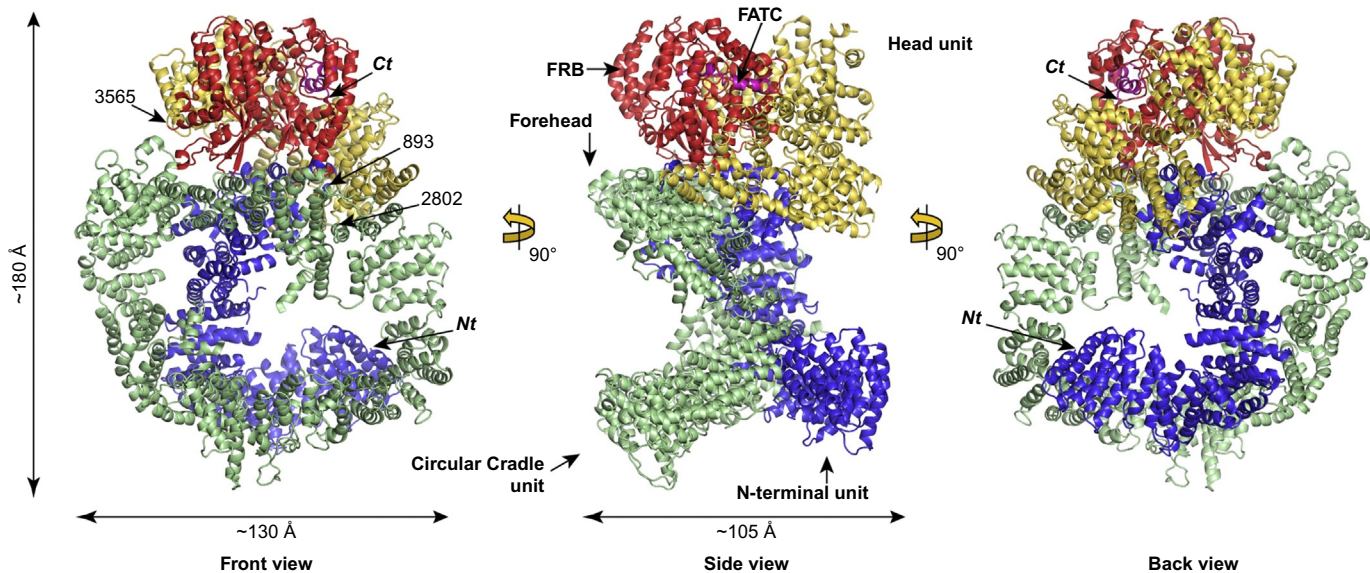


Fig. 5 The overall structure of DNA-PKcs. As in Fig. 1 structural units of DNA-PKcs are colored: N-terminal in blue, Circular Cradle in green, Head comprising FAT region in yellow, kinase in red, and the FATC in light pink. Also shown are the Forehead in light green and FRB (FKBP12-rapamycin-binding). Figure adapted from fig. 1 published in Sibanda, B.L., Chirgadze, D.Y., Ascher, D.B., Blundell, T.L. (2017). DNA-PKcs structure suggests an allosteric mechanism modulating DNA double-strand break repair. *Science*, 355(6324), 520–524. [<http://dx.doi.org/10.1126/science.aak9654>].

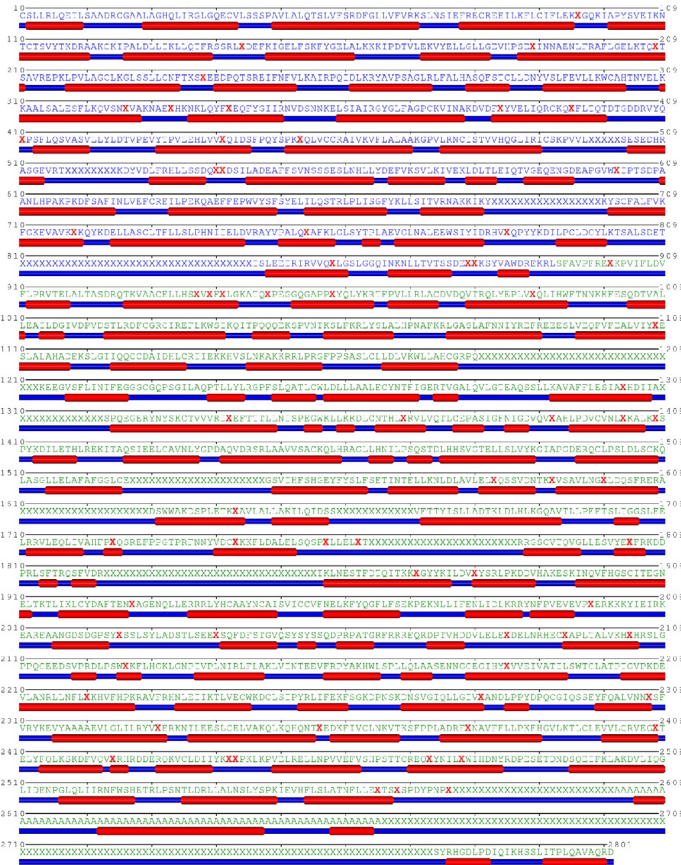


Fig. 6 Secondary structure assignment of the HEAT repeat rich regions—the N-terminal and Circular Cradle structural units of the DNA-PKcs crystal structure. The sequence is colored according to the schematic in Fig. 1. Here, α -helices are shown in red, loops in blue, and sheets in green. Residues not built into the electron density are shown by an X, and the location of Se-Met by bold red X's.

Apart from ensuring correct colocation at the appropriate time, we have argued that the complexity of such assemblies is in itself selectively advantageous (Blaszczyk, Harmer, Chirgadze, Ascher, & Blundell, 2015; Blundell et al., 2000; Bolanos-Garcia et al., 2012). Binary interactions in regulatory or signaling systems would occur opportunistically in the crowded environment of the cell, giving rise to noise in the system. However, cooperative formation of multiprotein systems would be less likely to form by chance, especially if they have many components and ordered-assembly mechanisms.

ACKNOWLEDGMENTS

Model coordinates have been deposited in the Protein Data Bank (PDB) under accession number 5LUQ.

We wish to thank Dr. Joop Van den Heuvel at Helmholtz-Zentrum and particularly Dr. Volker Jager who prepared the HeLa cells. We are also grateful to the ESRF (beamlines ID29, ID14-1, and ID14-2 in Grenoble, France) and DIAMOND (beamlines I04 and I03 in Oxford, UK) synchrotron sources where the data were collected. This work was funded by the Wellcome-Trust 093167/Z/10/Z. D.B.A is also funded by the Jack Brockhoff Foundation (JBF 4186, 2016) and a C. J. Martin Research Fellowship from the National Health and Medical Research Council of Australia (APP1072476).

REFERENCES

- Adams, P. D., Afonine, P. V., Bunkoczi, G., Chen, V. B., Davis, I. W., Echols, N., et al. (2010). PHENIX: A comprehensive python-based system for macromolecular structure solution. *Acta Crystallographica. Section D, Biological Crystallography*, 66(Pt. 2), 213–221.
- Bellizzi, J. J., Widom, J., Kemp, C. W., & Clardy, J. (1999). Producing selenomethionine-labeled proteins with a baculovirus expression vector system. *Structure*, 7(11), R263–R267.
- Blaszczak, M., Harmer, N. J., Chirgadze, D. Y., Ascher, D. B., & Blundell, T. L. (2015). Achieving high signal-to-noise in cell regulatory systems: Spatial organization of multiprotein transmembrane assemblies of FGFR and MET receptors. *Progress in Biophysics and Molecular Biology*, 118(3), 103–111.
- Blundell, T. L., Burke, D. F., Chirgadze, D., Dhanaraj, V., Hyvonen, M., Innis, C. A., et al. (2000). Protein-protein interactions in receptor activation and intracellular signalling. *Biological Chemistry*, 381(9–10), 955–959.
- Bolanos-Garcia, V. M., Wu, Q., Ochi, T., Chirgadze, D. Y., Sibanda, B. L., & Blundell, T. L. (2012). Spatial and temporal organization of multi-protein assemblies: Achieving sensitive control in information-rich cell-regulatory systems. *Philosophical Transactions. Series A, Mathematical Physical, and Engineering Sciences*, 370(1969), 3023–3039.
- Bowie, J. U., Luthy, R., & Eisenberg, D. (1991). A method to identify protein sequences that fold into a known three-dimensional structure. *Science*, 253(5016), 164–170.
- Buck, D., Malivert, L., de Chasseval, R., Barraud, A., Fondaneche, M. C., Sanal, O., et al. (2006). Cernunnos, a novel nonhomologous end-joining factor, is mutated in human immunodeficiency with microcephaly. *Cell*, 124(2), 287–299.
- Chen, B. P., Chan, D. W., Kobayashi, J., Burma, S., Asaithamby, A., Morotomi-Yano, K., et al. (2005). Cell cycle dependence of DNA-dependent protein kinase phosphorylation in response to DNA double strand breaks. *The Journal of Biological Chemistry*, 280(15), 14709–14715.
- Chiu, C. Y., Cary, R. B., Chen, D. J., Peterson, S. R., & Stewart, P. L. (1998). Cryo-EM imaging of the catalytic subunit of the DNA-dependent protein kinase. *Journal of Molecular Biology*, 284(4), 1075–1081.
- Critchlow, S. E., & Jackson, S. P. (1998). DNA end-joining: From yeast to man. *Trends in Biochemical Sciences*, 23(10), 394–398.
- Douglas, P., Cui, X., Block, W. D., Yu, Y., Gupta, S., Ding, Q., et al. (2007). The DNA-dependent protein kinase catalytic subunit is phosphorylated in vivo on threonine 3950, a highly conserved amino acid in the protein kinase domain. *Molecular and Cellular Biology*, 27(5), 1581–1591.
- Gell, D., & Jackson, S. P. (1999). Mapping of protein-protein interactions within the DNA-dependent protein kinase complex. *Nucleic Acids Research*, 27(17), 3494–3502.

- Grawunder, U., Wilm, M., Wu, X., Kulesza, P., Wilson, T. E., Mann, M., et al. (1997). Activity of DNA ligase IV stimulated by complex formation with XRCC4 protein in mammalian cells. *Nature*, 388(6641), 492–495.
- Hammel, M., Rey, M., Yu, Y., Mami, R. S., Classen, S., Liu, M., et al. (2011). XRCC4 protein interactions with XRCC4-like factor (XLF) create an extended grooved scaffold for DNA ligation and double strand break repair. *The Journal of Biological Chemistry*, 286(37), 32638–32650.
- Hammel, M., Yu, Y., Mahaney, B. L., Cai, B., Ye, R., Phipps, B. M., et al. (2010). Ku and DNA-dependent protein kinase dynamic conformations and assembly regulate DNA binding and the initial non-homologous end joining complex. *The Journal of Biological Chemistry*, 285(2), 1414–1423.
- Jubb, H. C., Higuieruelo, A. P., Ochoa-Montaño, B., Pitt, W. R., Ascher, D. B., & Blundell, T. L. (2017). Arpeggio: A web server for calculating and visualising interatomic interactions in protein structures. *Journal of Molecular Biology*, 429, 365–371.
- Leuther, K. K., Hammarsten, O., Kornberg, R. D., & Chu, G. (1999). Structure of DNA-dependent protein kinase: Implications for its regulation by DNA. *The EMBO Journal*, 18(5), 1114–1123.
- Li, Y., Chirgadze, D. Y., Bolanos-Garcia, V. M., Sibanda, B. L., Davies, O. R., Ahnesorg, P., et al. (2008). Crystal structure of human XLF/Cernunnos reveals unexpected differences from XRCC4 with implications for NHEJ. *The EMBO Journal*, 27(1), 290–300.
- Lieber, M. R. (2010). The mechanism of double-strand DNA break repair by the non-homologous DNA end-joining pathway. *Annual Review of Biochemistry*, 79, 181–211.
- Liu, Q., Zhang, Z., & Hendrickson, W. A. (2011). Multi-crystal anomalous diffraction for low-resolution macromolecular phasing. *Acta Crystallographica. Section D, Biological Crystallography*, 67(Pt. 1), 45–59.
- Meeck, K., Lees-Miller, S. P., & Modesti, M. (2012). N-terminal constraint activates the catalytic subunit of the DNA-dependent protein kinase in the absence of DNA or Ku. *Nucleic Acids Research*, 40(7), 2964–2973.
- Moshous, D., Callebaut, I., de Chasseval, R., Corneo, B., Cavazzana-Calvo, M., Le Deist, F., et al. (2001). Artemis, a novel DNA double-strand break repair/V(D)J recombination protein, is mutated in human severe combined immune deficiency. *Cell*, 105(2), 177–186.
- Ochi, T., Blackford, A. N., Coates, J., Jhujh, S., Mehmood, S., Tamura, N., et al. (2015). DNA repair. PAXX, a paralog of XRCC4 and XLF, interacts with Ku to promote DNA double-strand break repair. *Science*, 347(6218), 185–188.
- Ochi, T., Gu, X., & Blundell, T. L. (2013). Structure of the catalytic region of DNA ligase IV in complex with an Artemis fragment sheds light on double-strand break repair. *Structure*, 21(4), 672–679.
- Ochi, T., Sibanda, B. L., Wu, Q., Chirgadze, D. Y., Bolanos-Garcia, V. M., & Blundell, T. L. (2010). Structural biology of DNA repair: Spatial organisation of the multicomponent complexes of nonhomologous end joining. *Journal of Nucleic Acids 2010*, Article ID 621695, 19 pages. <http://dx.doi.org/10.4061/2010/621695>.
- Ochi, T., Wu, Q., Chirgadze, D. Y., Grossmann, J. G., Bolanos-Garcia, V. M., & Blundell, T. L. (2012). Structural insights into the role of domain flexibility in human DNA ligase IV. *Structure*, 20(7), 1212–1222.
- O'Driscoll, M., & Jeggo, P. A. (2006). The role of double-strand break repair - insights from human genetics. *Nature Reviews. Genetics*, 7(1), 45–54.
- Rivera-Calzada, A., Maman, J. D., Spagnolo, L., Pearl, L. H., & Llorca, O. (2005). Three-dimensional structure and regulation of the DNA-dependent protein kinase catalytic subunit (DNA-PKcs). *Structure*, 13(2), 243–255.
- Schatz, D. G. (2004). V(D)J recombination. *Immunological Reviews*, 200, 5–11.

- Sibanda, B. L., Chirgadze, D. Y., Ascher, D. B., & Blundell, T. L. (2017). DNA-PKcs structure suggests an allosteric mechanism modulating DNA double-strand break repair. *Science*, *355*(6324), 520–524. <http://dx.doi.org/10.1126/science.aak9654>.
- Sibanda, B. L., Chirgadze, D. Y., & Blundell, T. L. (2010). Crystal structure of DNA-PKcs reveals a large open-ring cradle comprised of HEAT repeats. *Nature*, *463*(7277), 118–121.
- Sibanda, B. L., Critchlow, S. E., Begun, J., Pei, X. Y., Jackson, S. P., Blundell, T. L., et al. (2001). Crystal structure of an Xrcc4-DNA ligase IV complex. *Nature Structural Biology*, *8*(12), 1015–1019.
- Singleton, B. K., Torres-Arzuayus, M. I., Rottinghaus, S. T., Taccioli, G. E., & Jeggo, P. A. (1999). The C terminus of Ku80 activates the DNA-dependent protein kinase catalytic subunit. *Molecular and Cellular Biology*, *19*(5), 3267–3277.
- Smith, R. E., Lovell, S. C., Burke, D. F., Montalvao, R. W., & Blundell, T. L. (2007). Andante: Reducing side-chain rotamer search space during comparative modeling using environment-specific substitution probabilities. *Bioinformatics*, *23*(9), 1099–1105.
- Spagnolo, L., Rivera-Calzada, A., Pearl, L. H., & Llorca, O. (2006). Three-dimensional structure of the human DNA-PKcs/Ku70/Ku80 complex assembled on DNA and its implications for DNA DSB repair. *Molecular Cell*, *22*(4), 511–519.
- Villarreal, S. A., & Stewart, P. L. (2014). CryoEM and image sorting for flexible protein/DNA complexes. *Journal of Structural Biology*, *187*(1), 76–83.
- Walker, J. R., Corpina, R. A., & Goldberg, J. (2001). Structure of the Ku heterodimer bound to DNA and its implications for double-strand break repair. *Nature*, *412*(6847), 607–614.
- Weterings, E., Verkaik, N. S., Keijzers, G., Florea, B. I., Wang, S. Y., Ortega, L. G., et al. (2009). The Ku80 carboxy terminus stimulates joining and artemis-mediated processing of DNA ends. *Molecular and Cellular Biology*, *29*(5), 1134–1142.
- Willard, L., Ranjan, A., Zhang, H., Monzavi, H., Boyko, R. F., Sykes, B. D., et al. (2003). VADAR: A web server for quantitative evaluation of protein structure quality. *Nucleic Acids Research*, *31*(13), 3316–3319.
- Williams, D. R., Lee, K. J., Shi, J., Chen, D. J., & Stewart, P. L. (2008). Cryo-EM structure of the DNA-dependent protein kinase catalytic subunit at subnanometer resolution reveals alpha helices and insight into DNA binding. *Structure*, *16*(3), 468–477.
- Wu, Q., Ochi, T., Matak-Vinkovic, D., Robinson, C. V., Chirgadze, D. Y., & Blundell, T. L. (2011). Non-homologous end-joining partners in a helical dance: Structural studies of XLF-XRCC4 interactions. *Biochemical Society Transactions*, *39*(5), 1387–1392. Suppl. 1382 p following 1392.